

Vibrational Spectra of Tetracyano-1,4-dithiin

Jiro NAKANISHI*† and Tohru TAKENAKA*

Received May 1, 1978

Infrared spectra of the tetracyano-1,4-dithiin (TCND) crystal were recorded at the normal incidence of polarized radiation upon the (010) sample plane at various angles between the electric vector of the incident radiation and the *a* crystal axis from 0° to 180°. Polarized Raman spectra of the crystal were also recorded. The depolarization ratios of the Raman bands were obtained in solutions. From the results obtained, the infrared and Raman bands were classified into four symmetry species of the C_{2v} molecular group under the assumption of the oriented gas model. Assignments of the observed bands to the individual fundamental vibrations were carried out with the aid of the above-mentioned examinations, the spectral data of analogous molecules, and the normal coordinate analysis.

INTRODUCTION

In the previous work, the present authors have studied the infrared and Raman spectra of tetracyanothiophene (TCNT)¹⁾ as the first work in a series of vibrational studies of the thiacyano compounds. This paper deals with the details of vibrational spectra of tetracyano-1,4-dithiin (TCND), from which TCNT is easily prepared.

Polarized infrared spectra of the TCND crystal with the (010) crystal plane were recorded at various angles between the electric vector of the polarized radiation and the *a* crystal axis. From the results obtained, the observed bands were classified into three infrared-active species a_1 , b_1 , and b_2 of the C_{2v} molecular group. The far-infrared spectrum was recorded for the powdered sample. Polarized Raman spectra of the crystal were recorded for the two optical geometries which are free from effects of birefringence. Raman spectra of the solutions were also recorded and the depolarization ratios of the Raman bands were determined. The results thus obtained regarding the classification of the Raman bands were consistent with those obtained for corresponding infrared bands.

Assignments of the observed bands to the individual fundamental modes were carried out with the aid of the above-mentioned examinations, the spectral data of analogous molecules, and the normal coordinate analysis carried out by using the modified Urey-Bradley force field. Agreements between the calculated and observed frequencies were satisfactory except for a few low-frequency bands, which are presumably coupled with lattice vibrations.

EXPERIMENTAL

A sample of TCND was prepared by the method of Simmons and his cowork-

* 中西次郎, 竹中 亨: Laboratory of Surface Chemistry, Institute for Chemical Research, Kyoto University, Uji, Kyoto, 611.

† Present address: Sasakura Engineering Co., Ltd., 7-5, Mitejima, 6-Chome, Nishiyodogawa-ku, Osaka, 555.

ers.²⁾ Disodium dimercaptomaleonitrile was oxidized with thionyl chloride and the product was recrystallized at first from toluene and then from 1,2-dichloroethane. Infrared and ultraviolet spectra of the pale yellow crystal thus obtained were identical with those reported previously.²⁾

The crystal structure of TCND has been reported by Dollase³⁾ to be the monoclinic system, $a=6.953$, $b=18.498$, $c=7.024$ Å, and $\beta=90.52^\circ$, with a space group $P2_1/n-C_{2h}^5$ with four molecules in a unit cell. The X-ray diffraction studies indicated that the crystal obtained from 1,2-dichloroethane solution had the same crystal form as that reported by Dollase,³⁾ while the crystal obtained from toluene solution had a different form.⁴⁾

The thin crystal sample of 4×8 mm for infrared measurements was prepared as follows. The crystal was pasted on a KBr plate with Araldite keeping the (010) plane parallel to the KBr plate and polished with a silk cloth containing dichloromethane until a suitable thickness was achieved. Infrared spectra of this crystal were recorded at the normal incidence of polarized radiation by varying the angle θ between the electric vector of the incident radiation and the a crystal axis from 0° to 180° . Polarized infrared spectra between 4000 and 250 cm^{-1} were recorded on a Perkin-Elmer model 521 grating spectrophotometer equipped with a wire grid polarizer.

For measurements of the far-infrared spectrum of the powdered sample, a Hitachi model FIS-3 vacuum grating spectrophotometer was used. The polarization measurements could not be made because the sample crystal with area large enough for far-infrared measurements could not be obtained.

For polarization measurements of Raman spectra, a crystal of $1 \times 1 \times 2$ mm was cut in a parallelepipedon along the a , b , and c axes. In this experiment, considerable difference of the spectra was found between, for example, the $a(ca)b$ and $b(ac)a$ geometries (expressed by Porto's notation⁵⁾), which should be identical if the effects of birefringence are negligible. This fact therefore suggests that the effects of birefringence are considerable in this crystal. It is known that in case of the monoclinic system one of the principal axes of the index ellipsoid is parallel to the b axis and other two (a^* and c^*) axes are perpendicular to it.⁶⁾ For the crystal sample mentioned above, only three spectra expressed by the (ba^*) , (bc^*) , and (bb) may be obtained without the effects of birefringence. However, a reliable spectrum of the (bb) geometry could not be recorded because a clean (001) surface was hardly obtained.

Raman spectra of saturated solution were observed in 1,2-dichloroethane, acetonitrile, N,N-dimethylformamide, and acetone at 40° or 60°C . Raman spectra were recorded on a Japan Electron Optics Laboratory model JRS-S1 spectrophotometer equipped with a Spectra Physics model 164-03 Ar ion laser and model 164-01 Kr ion laser. A Glan-Thomson prism and polaroid were used for polarization measurements.

SELECTION RULES

The TCND molecule has been reported to be in a folded structure with dihedral angle of 124° and have the C_{2v} symmetry.³⁾ The selection rules for the free molecule

Table I. Correlation Diagram and Selection Rules^{a)} of TCND

Molecular group C_{2v}	Site group C_1	Factor group C_{2h}^2
10 a_1 (R, p and IR, $M_x^{b)}$	36 A	36 A_g (R, $\alpha_{aa}, \alpha_{bb}, \alpha_{cc}, \alpha_{ca}$)
9 a_2 (R, dp)		36 B_g (R, α_{ab}, α_{bc})
8 b_1 (R, dp and IR, $M_x^{b)}$		36 A_u (IR, M_b)
9 b_2 (R, dp and IR, $M_y^{b)}$		36 B_u (IR, M_{ac})

- a) R, Raman-active; IR, infrared-active; p , polarized; dp , depolarized.
 b) For the molecular-fixed axes x, y , and z , see Fig. 5.

and those for the molecules in the crystal are given in the correlation diagram of Table I, suggesting that each vibration of the free molecule splits in the crystal into four modes: two are infrared-active and remaining two are Raman-active. The infrared bands observed at the normal incidence of radiation upon the (010) crystal plane belong to the B_u species of the factor group, and the Raman bands observed at the (ba^*) and (bc^*) geometries belong to the B_g species.

INFRARED AND RAMAN SPECTRA

Figure 1 represents the polarized infrared spectra of the crystal with the (010) plane. The solid, broken, and dotted lines refer to the spectra obtained at the θ values of 0° , 60° , and 100° , respectively.

In order to classify the observed infrared bands into the three infrared-active species a_1 , b_1 , and b_2 , the change in observed band-intensities with the angle θ was compared with the corresponding theoretical curves, which were obtained from the crystal data³⁾ under the assumption of the oriented gas model. The results are shown in Fig. 2. The solid, broken, and dotted lines are the theoretical curves for

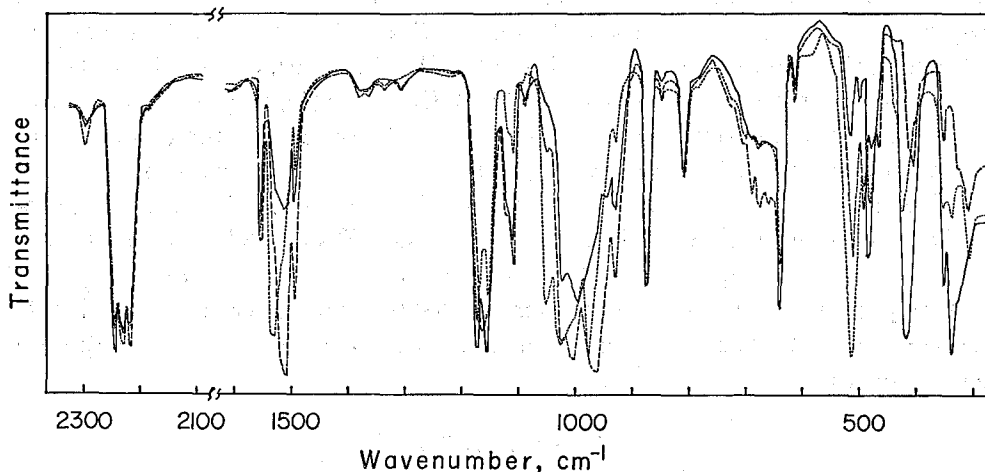


Fig. 1. Polarized infrared spectra of the TCND crystal with the (010) plane.
 —: $\theta=0^\circ$, ----: $\theta=60^\circ$,: $\theta=100^\circ$.

Vibrational Spectra of TCND

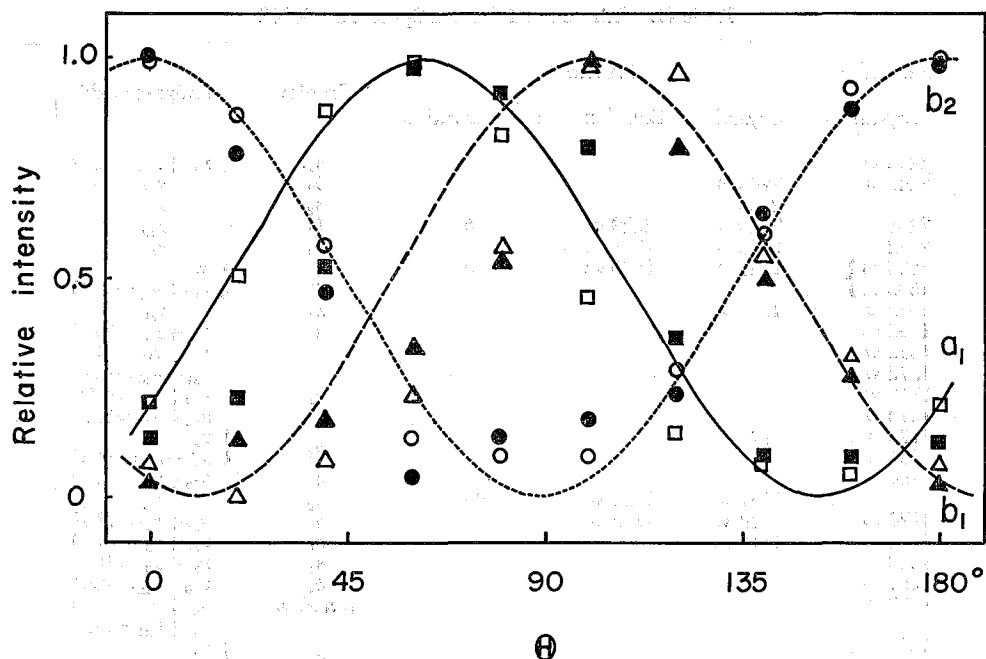


Fig. 2 Relative intensities of the infrared bands as a function of the angle θ at 1528(\blacktriangle), 1505(\square), 1051(\triangle), 495(\blacksquare), 430(\circ), and 353 cm^{-1} (\bullet).

the a_1 , b_1 , and b_2 species, respectively. Observed band-intensities were normalized in such a way that the maximum value of each band is unity. There are considerable departures of the experimental values from the theoretical curves. This is probably due to imperfection of the crystal and the effects of birefringence. However,

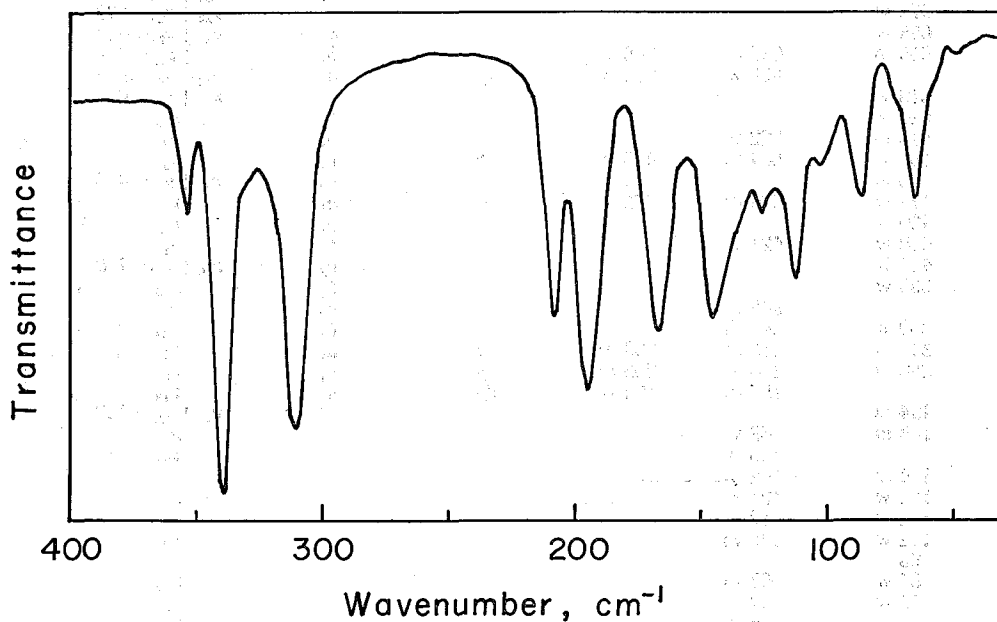


Fig. 3. Far-infrared spectrum of the TCND powder.

Table II. Infrared and Raman Spectra of TCND

Infrared ^{a)}		Raman ^{a)}		Species	Assignments ^{b)}
Crystal	Crystal	Solution	Depolarization		
2298 w				a_1	$\nu_1 + \nu_{10} = 2288$
2246 s	2243 s			b_2	ν_{28}
	2235 s			a_2	ν_{11}
2231 s	2229 s	2229 m	dp	b_1	ν_{20}
2222 s	2219 s	2218 vs	p	a_1	ν_1
1556 m	1561 s	1560 vs	p	a_1	{ ν_2 $\nu_{29} + \nu_{33} = 1525$
1505 vs				b_1	
1528 s	1521 w			a_1	ν_{21}
1495 m				a_1	$\nu_3 + \nu_5 = 1490$
1385 w					$\nu_8 + \nu_{29} = 1381$
1372 w					$\nu_{21} - \nu_{26} = 1372$
1340 w				a_1	$\nu_{29} + \nu_{35} = 1338$
1310 w					$\nu_{12} + \nu_{26} = 1310$
1176 s	1178 w			b_2	{ ν_{29} $\nu_3 + \nu_{35} = 1156$
1154 s				a_1	
1164 m				a_1	$\nu_{30} + \nu_{35} = 1160$
	1157 w	1150 w	dp	a_2	ν_{12}
1124 sh	1128 w	1122 w	p	a_1	$\nu_{22} + \nu_{26} = 1137$
1112 m	1116 sh			a_1	$\nu_{31} + \nu_{35} = 1110$
1088 w				a_1	$\nu_3 + \nu_9 = 1092$
1051 m				b_1	$\nu_{10} + \nu_{22} = 1051$
1023 s				a_1 and b_1	$\nu_4 + \nu_5 = 1019$
					$\nu_5 + \nu_{23} = 1024$
1001 vs				a_1	{ ν_3 $\nu_4 + \nu_6 = 990$
978 vs				b_2	
994 s				b_1	ν_{30}
984 s				b_2	ν_{22}
944 w				b_2	ν_{31}
931 w				a_1	$\nu_{30} - \nu_{36} = 935$
872 m				a_1	$\nu_4 + \nu_{33} = 872$
852 w				a_1	$2 \times \nu_{32} = 860$
	845 w			a_2	{ ν_{14} $\nu_{30} - \nu_{26} = 841$
	832 w				
810 w					$\nu_5 + \nu_7 = 814$
690 w				a_1	$\nu_{33} + \nu_{34} = 693$
676 w				a_1	$\nu_{23} + \nu_{26} = 677$
658 w				a_1	$\nu_{23} + \nu_{27} = 648$
645 m	645 m	645 w	dp	b_2	$\nu_8 + \nu_{32} = 639$
	620 w	615 w	dp	a_2	$\nu_{14} - \nu_8 = 630$
					$\nu_{18} + \nu_{25} = 616$
616 w				b_1	ν_{23}
524 s				a_1	ν_4
516 m	522 w			a_1	ν_5
495 w	504 m	495 s	p	b_2	$\nu_7 + \nu_{35} = 480$
480 m				a_1	ν_6
472 w	470 m	465 s	p	b_2	ν_{32}
430 s				b_1	ν_{25}
418 w	421 w			b_2	$\nu_{10} + \nu_{33} = 420$
412 w				b_2	ν_{33}
353 w				a_2	ν_{16}
	349 m			b_2	ν_{34}
339 s	340 m			a_1	ν_7
311 m	316 m	300 m	p	a_1	ν_8
208 m	210 s	205 m	p	a_1	ν_{18}
	196 m	190 w	dp	a_2	$\nu_{19} + \nu_{26} = 198$
194 m					ν_{35}
168 m	163 w				ν_{26}
	153 s				
	142 s				
144 m	121 w				ν_{27}
126 w	112 w				
112 w	102 vs				ν_9
102 w					
86 w					
65 w	68 vs				ν_{10}
58 w	59 s				ν_{36}
	45 s				ν_{19}

a) vs, very strong; s, strong; m, medium; w, weak.

b) See Table 4.

Vibrational Spectra of TCND

a glance at the overall θ -dependence of the observed intensities leads to unambiguous classifications of the most observed bands into the three infrared-active species.

The bands at 1556, 872, 810, and 616 cm^{-1} showed little intensity change with change in the θ value. This may be due to the overlap of, at least, two bands belonging to the different species. Figure 3 represents the far-infrared spectrum of the powdered sample. The infrared and far-infrared data are summarized in Table II.

Raman spectra of TCND in acetone are shown in Fig. 4A. The bands marked with arrows are due to the solvent. Effects of the solvents on the bands frequencies of TCND were scarcely observed. The solid and broken lines refer to the Raman scattering with the electric vector parallel and perpendicular to that of the exciting light, respectively. The bands at 2218, 1560, 1122, 495, 465, 300, and 205 cm^{-1} were found to be polarized and attributed to the totally symmetric (a_1) vibrations.

The proportionality factors for Raman intensities of the crystal at the (ba^*) and (bc^*) geometries are shown in Table III, as obtained from the crystal data³⁾ under

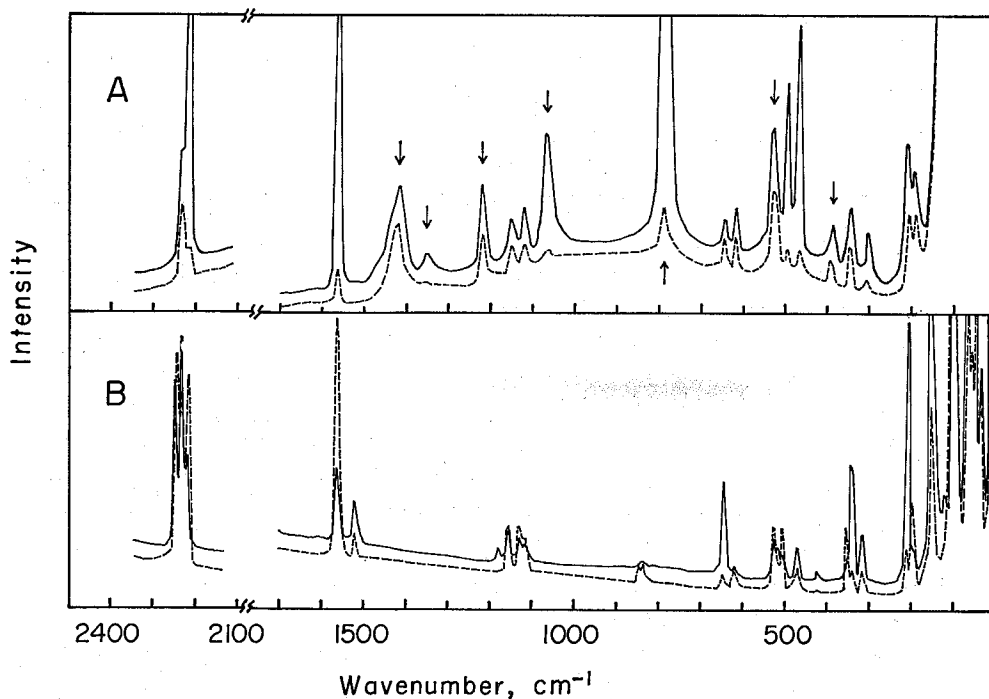


Fig. 4. [A] Raman spectra of TCND in acetone. Bands marked with arrows are due to the solvent. —: $I_{//}$, ----: I_{\perp} .

[B] Raman spectra of the TCND crystal. —: $a(ba^*)b$, ----: $a(bc^*)b$.

Table III. Proportionality Factors of Raman Intensities

Geometry	a_2	b_1	b_2
(ba^*)	0.05	0.20	0.44
(bc^*)	0.21	0.04	0.06

the assumption of the oriented gas model. It is expected from this table that the bands of the a_2 species are stronger at the (bc^*) geometry, while those of the b_1 and b_2 species are stronger at the (ba^*) geometry. Furthermore, the bands of the b_2 species are expected to be much stronger at the (ba^*) geometry as compared with those of the b_1 species.

Polarized Raman spectra of this crystal are given in Fig. 4B. The solid and broken lines refer to the spectra obtained by the $a(ba^*)b$ and $a(bc^*)b$ geometries, respectively. From the expectation mentioned above, the bands at 2235, 1157, 845, 832, 620, 349, and 196 cm^{-1} were classified into the a_2 species. Those at 1178, 645, and 340 cm^{-1} seem to belong to the b_2 species. The bands at 2243, 2229, and 421 cm^{-1} could be classified into either of the b_1 and b_2 species, however, it is difficult to select one of those species because of the overlap with other bands or very weak intensities. Therefore, these bands were classified into the b_1 or b_2 species from the results of the corresponding infrared bands. The results are also given in Table II.

ASSIGNMENTS

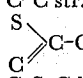
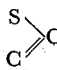
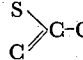
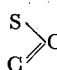
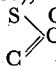
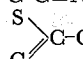
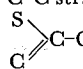
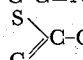
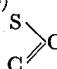
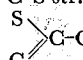
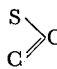
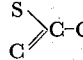
In order to make assignments of the observed bands to the individual fundamental modes, the following examinations were carried out besides the discussions in the previous section: (a) A comparison of the spectral data with those of the partly analogous molecules, such as TCNT,¹⁾ the bis-(1,2-dicyanoethylene-1,2-dithiolato) niccolate (II) anion,⁷⁾ TCNE,^{8~14)} TCNQ,^{15~18)} and TCNB.^{19,20)} (b) The normal coordinate analysis mentioned in the next section. In the following discussions, the mean values of the infrared and Raman frequencies of the crystal were used as the fundamental frequencies, when both were observed.

In the region from 2250 to 2200 cm^{-1} , four fundamental $\text{C}\equiv\text{N}$ stretching vibrations are expected. The Raman bands due to the $\text{C}\equiv\text{N}$ stretching vibration were observed at 2243, 2235, 2229, and 2219 cm^{-1} for the crystal. The infrared bands at 2246, 2231, and 2222 cm^{-1} correspond to the Raman bands at 2243, 2229, and 2219 cm^{-1} , respectively, and have already been assigned to the b_2 , b_1 , and a_1 vibrations, respectively. Very strong Raman band at 2218 cm^{-1} in solution is apparently polarized. The Raman bands at 2235 cm^{-1} has also been assigned to the a_2 vibration previously. The fact that there is no infrared band corresponding to this Raman band is consistent with this assignment.

In the region of 1500 cm^{-1} , two fundamental $\text{C}=\text{C}$ stretching vibrations of the a_1 and b_1 species are expected. The Raman bands in this region were observed at 1561 and 1521 cm^{-1} for the crystal, and may be assigned to these vibrations. Since the 1561- cm^{-1} band corresponds to a strong and highly polarized band at 1560 cm^{-1} in solution, it can be assigned to the a_1 vibration and therefore the 1521- cm^{-1} band to the b_1 vibration. The infrared bands were observed at 1556, 1528, 1505, and 1495 cm^{-1} . The 1556- and 1505- cm^{-1} bands of the a_1 species may be due to the Fermi resonance between the fundamental vibration and combination tone ($\nu_{29} + \nu_{33} = 1525 \text{ cm}^{-1}$). The 1528- cm^{-1} band of the b_1 species corresponds to the Raman band at 1521 cm^{-1} mentioned above. The remaining band at 1495 cm^{-1} was assigned to the combination tone ($\nu_3 + \nu_5 = 1490 \text{ cm}^{-1}$).

Vibrational Spectra of TCND

Table IV. Fundamental Vibrations of TCND

Symmetry species	Observed freq. (cm ⁻¹)	Calcd. freq. (cm ⁻¹)	Dev. ^{a)} (%)	P.E.D. (%) ^{b),c)}	
<i>a</i> ₁	ν_1	2221	2235	0.6	C≡N str. (87)
	ν_2	1546	1544	-0.1	C=C str. (70)
	ν_3	990	1018	2.8	C-C str. (53), C-S str. (38)
	ν_4	519	517	-0.4	 C-CN def. (48), C-C≡N def. (30)
	ν_5	500	506	1.2	C-S-C bend. (25)
	ν_6	471	458	-2.8	C-S str. (35)
	ν_7	314	309	-1.6	C-C≡N' def. (52), C-S-C bend. (33)
	ν_8	209	209	0.0	C-S torsion (34)
	ν_9	102	119	16.7	C-C≡N def. (60),  C-C-CN def. (29)
	ν_{10}	67	56	-16.4	 C-CN' def. (72)
<i>a</i> ₂	ν_{11}	2235	2230	-0.2	C≡N str. (88)
	ν_{12}	1157	1141	-1.4	C-C str. (32), C-S str. (31)
	ν_{13}	—	907	—	C-C str. (45)
	ν_{14}	839	840	0.1	C=C torsion (39),  C-C-CN' def. (33)
	ν_{15}	—	494	—	C-S str. (38),  C-C-CN def. (36)
	ν_{16}	349	345	-1.1	C-C≡N' def. (88)
	ν_{17}	—	238	—	C=C-S bend. (66)
	ν_{18}	196	195	-0.5	C-C≡N def. (68)
	ν_{19}	45	45	0.0	 C-C-CN' def. (66)
<i>b</i> ₁	ν_{20}	2230	2234	0.2	C≡N str. (87)
	ν_{21}	1525	1530	0.3	C=C str. (73)
	ν_{22}	984	972	-1.2	C-C str. (56), C-S str. (36)
	ν_{23}	524	523	-0.2	 C-CN def. (41), C-S str. (30)
	ν_{24}	—	504	—	C-S str. (25)
	ν_{25}	420	427	1.7	C-C≡N' def. (77)
	ν_{26}	153	154	0.7	 C-C-CN' def. (76)
	ν_{27}	124	125	0.8	C-C≡N def. (65),  C-C-CN def. (34)
<i>b</i> ₂	ν_{28}	2245	2230	-0.7	C≡N str. (88)
	ν_{29}	1172	1183	0.9	C-S str. (32), C-C str. (31)
	ν_{30}	994	996	0.2	C-S torsion (36), C=C torsion (30)
	ν_{31}	944	939	-0.5	C-C str. (38)
	ν_{32}	430	440	2.3	C-S str. (38), C-C≡N def. (32),  C-C-CN def. (25)
	ν_{33}	353	356	0.8	C-C≡N' def. (89)
	ν_{34}	340	341	0.3	C=C-S bend. (47)
	ν_{35}	166	165	-0.6	C-C≡N def. (59),  C-C-CN def. (28)
	ν_{36}	59	58	-1.7	 C-C-CN' def. (71)

a) Dev. = 100 [$\nu(\text{Calcd}) - \nu(\text{Obsd.})$]/ $\nu(\text{Obsd.})$.

b) Only contributions greater than 25 per cent are included.

c) The prime (') on the N atom refer to the out-of-plane vibration.

In the region from 1200 to 900 cm^{-1} , the six fundamental bands (ν_3 , ν_{12} , ν_{13} , ν_{22} , ν_{29} , and ν_{31}) due to the C-S and C-C stretching vibrations, and one torsional band ν_{30} are expected. Two very strong infrared bands of the a_1 species at 1001 and 978 cm^{-1} seem to be due to the Fermi resonance between the ν_3 vibration and the combination tone ($\nu_4 + \nu_6 = 990 \text{ cm}^{-1}$). The Raman band due to the ν_{12} vibration (the a_2 species) was observed at 1157 cm^{-1} , but any band assignable to the ν_{13} vibration of the a_2 species could not be observed in this region. The infrared bands of the b_1 species were observed at 1051, 1023, and 984 cm^{-1} . The strongest one at 984 cm^{-1} was assigned to the ν_{22} vibration and other bands to the combination tones as shown in Table II. The Raman band of the b_2 species was observed at 1178 cm^{-1} and was assigned to the ν_{29} vibration. The corresponding infrared band may be the doublet bands at 1176 and 1154 cm^{-1} which are due to the Fermi resonance between the ν_{29} and the combination tone ($\nu_3 + \nu_{35} = 1156 \text{ cm}^{-1}$). The bands at 994 and 944 cm^{-1} of the b_2 species were easily assigned to the ν_{30} and ν_{31} vibrations, respectively.

With the aid of the experimental results and the normal coordinate analysis, remaining lower frequency bands could be assigned without serious difficulties. The results of these discussions are summarized in the last column of Table II. The frequencies of the fundamental vibrations are listed in Table IV.

NORMAL COORDINATE ANALYSIS

Wilson's GF matrix method²¹⁾ was used for the normal coordinate analysis. The numerical calculations were carried out with the aid of a FACOM 230 OSII/VS of this institute. The internal coordinates are given in Fig. 5. The equilibrium bond lengths adopted are the mean values of those determined by Dollase:³⁾

$$L_1^0 = L_2^0 = L_3^0 = L_4^0 = 1.755 \text{ \AA}, \quad l_5^0 = l_6^0 = l_7^0 = l_8^0 = 1.432 \text{ \AA}, \\ r_9^0 = r_{10}^0 = r_{11}^0 = r_{12}^0 = 1.150 \text{ \AA}, \quad R_{13}^0 = R_{14}^0 = 1.344 \text{ \AA}.$$

For the bond angles, $\alpha_1^0 = \alpha_2^0 = 97.3^\circ$ was used as reported by Dollase, while $\alpha_3^0 = \alpha_4^0 = \dots = \alpha_{14}^0 = 120^\circ$ and $\alpha_{15}^0 = \alpha_{16}^0 = \alpha_{17}^0 = \alpha_{18}^0 = 180^\circ$ were assumed for the sake of simplicity.

As the potential function for the TCND molecule, the modified Urey-Bradley force field (mod. UBFF) given by:

$$V(\text{mol. UBFF}) = V(\text{UBFF}) \\ + C(\text{S}\cdots\text{S})(\Delta q_1)^2 + 2C'(\text{S}\cdots\text{S})(\Delta q_1)q_1^0 \\ + \sum_{i=2}^3 \left[\frac{1}{2} C(\text{C}\cdots\text{C})(\Delta q_i)^2 + C'(\text{C}\cdots\text{C})(\Delta q_i)q_i^0 \right] \\ + \sum_{i=1}^4 \alpha(\Delta L_i)(\Delta l_{i+4})$$

was used. Here, q_i^0 is the equilibrium *cis* non-bonded distance between two sulfur atoms and q_i^0 's ($i=2$ and 3) are those between two carbon atoms (Fig. 5). Force constants $C(\text{S}\cdots\text{S})$ and $C(\text{C}\cdots\text{C})$ are the coefficients of respective repulsion terms

Vibrational Spectra of TCND

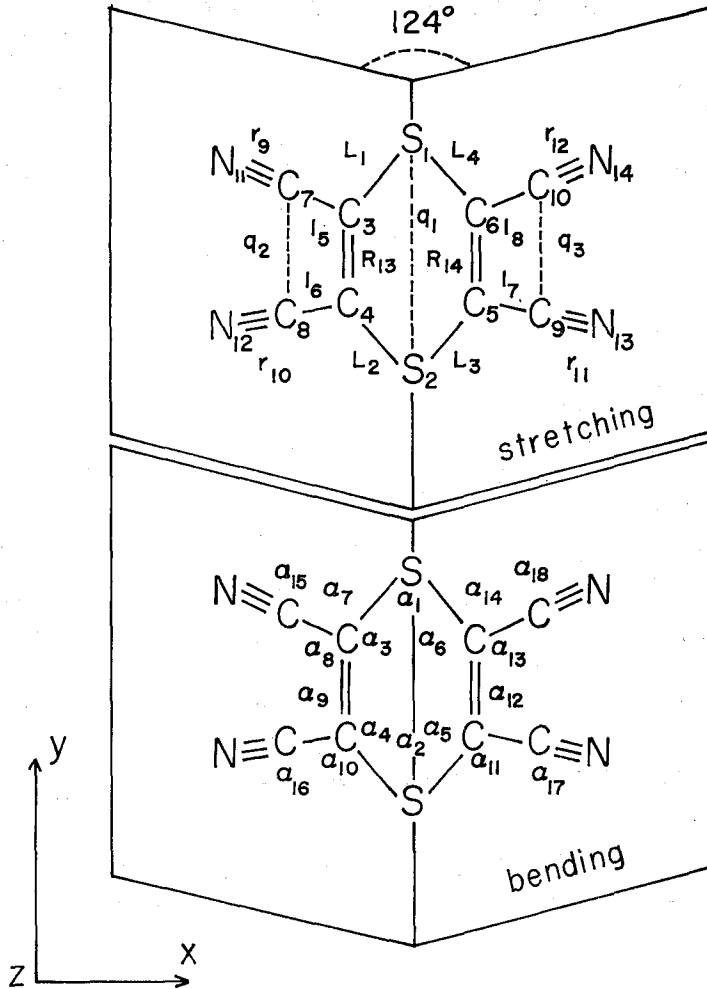


Fig. 5. Internal coordinates of TCND.

and α the coefficient of the cross terms between the C-S and C-C stretching coordinates. $V(\text{UBFF})$ consists of terms with four bond-stretching, seven-bending, four non-bonded repulsion, and two torsional force constants; those constants are listed in the first column of Table V.

For the first calculation, the force constants were transferred from TCNT.¹⁾ After some refinements of the values by the trial-and-error method using Jacobian matrix, repetitions of the calculations with several sets of the force constants were carried out by the least-squares method. In these calculations the values of two force constants $K(\text{C-S})$ and α were fixed at 3.52 and 0.73 mdyne/Å, respectively, to have the converged set of the force constants. These values were determined to obtain better agreement between the observed and calculated frequencies. The converged set of the force constants thus obtained are shown in Table V, together with their dispersion values. The calculated frequencies with this set of the force

Table V. Force Constants^{a)} (mdyne/Å) of TCND

	Force Constant	Dispersion
$K(\text{C-S})$	3.52	— ^{b)}
$K(\text{C-C})$	4.80	0.36
$K(\text{C}\equiv\text{N})$	17.12	0.58
$K(\text{C=C})$	6.10	0.36
$H(\text{C-S-C})$	0.15	0.12
$H(\text{C=C-S})$	0.08	0.23
$H(\text{C-C-S})$	0.36	0.19
$H(\text{C=C-C})$	0.32	0.25
$H(\text{C-C}\equiv\text{N}, \text{in-plane})$	0.15	0.01
$H\left(\begin{array}{c} \text{S} \\ \diagup \\ \text{C} \end{array} \right) \text{C-CN}, \text{out-of-plane}$	0.20	0.01
$H(\text{C-C}\equiv\text{N}, \text{out-of-plane})$	0.17	0.01
$F(\text{C-S-C})$	0.56	0.21
$F(\text{C=C-S})$	—0.01	0.67
$F(\text{C-C-S})$	0.01	0.28
$F(\text{C=C-C})$	0.43	0.85
$T(\text{C-S})$	0.39	0.14
$T(\text{C=C})$	0.42	0.12
$C(\text{S}\cdots\text{S})$	—0.09	0.08
$C(\text{C}\cdots\text{C})$	0.23	0.12
α	0.73	— ^{b)}

a) The $F' = -0.1F$ and $C' = -0.1C$ relations were assumed.

b) Fixed.

constants are compared with the observed values in Table IV. The agreement is satisfactory except for a few low-frequency bands, which are presumably coupled with lattice vibrations. The last column of Table IV represents the potential energy distribution.

The stretching force constants given in Table V seem to be reasonable. The value of the force constant $K(\text{C-S})$ is smaller than that of TCNT (4.15 mdyne/Å) and the value of $K(\text{C=C})$ is larger than that of TCNT (5.60 mdyne/Å). This fact suggests that the delocalization of the electrons in the ring of TCND is less than that in the ring of TCNT. This is understandable by considering that the TCND molecule has the folded structure with the dihedral angle of 124°, while the TCNT molecule is the plane molecule. On the other hand, comparing the present values obtained for $K(\text{C-C})$ and $K(\text{C}\equiv\text{N})$ with their usual values of non-resonant systems, it is apparent that the C-C bond still acquires the partial double-bond character and the C≡N bond loses the triple-bond character. It is, therefore, inferred that the resonance effect is appreciable for the S-C=C-C≡N group in each plane of the folded TCND molecule.

ACKNOWLEDGMENT

The authors express their gratitude to Professor Sinzaburo Oka of this institute for guidance in preparation of the TCND samples. Thanks are also due to Professor

Vibrational Spectra of TCND

Soichi Hayashi and Dr. Junzo Umemura of this laboratory for their helpful discussions during the course of this work.

REFERENCES

- (1) J. Nakanishi and Tohru Takenaka, *Bull. Chem. Soc. Japan.*, **50**, 36 (1977).
- (2) H.E. Simmons, R.D. Vest, D.C. Blomstrom, J.R. Roland, and T.L. Cairns, *J. Am. Chem. Soc.*, **84**, 4746 (1962).
- (3) W.A. Dollase, *J. Am. Chem. Soc.*, **87**, 979 (1965).
- (4) The crystal obtained from toluene solution was found to contain the solvent molecules, which were released gradually in the air. As a result of this, the crystal became an amorphous solid.
- (5) T.C. Damen, S.P.S. Porto, and S.B. Tell, *Phys. Rev.*, **142**, 570 (1966).
- (6) The a^* and c^* principal axes of the index ellipsoid were determined by means of a polarization microscope.
- (7) Lakshmi, P.B. Rao, and U. Agarwala, *Appl. Spectroscopy*, **25**, 207 (1971).
- (8) D.A. Long and W.O. George, *Spectrochim. Acta*, **19**, 1717 (1963).
- (9) T. Takenaka and S. Hayashi, *Bull. Chem. Soc. Japan.*, **37**, 1216 (1964).
- (10) F.A. Miller, O. Sala, P. Devlin, J. Overend, E. Lippert, W. Lüder, H. Moser, and J. Varchmin, *Spectrochim. Acta*, **20**, 1233 (1964).
- (11) A. Rosenberg and J.P. Devlin, *Spectrochim. Acta*, **21**, 1613 (1965).
- (12) Von P. Heim and F. Dörr, *Ber. Bunsenges. Phys. Chem.*, **69**, 453 (1965).
- (13) J. Stanley, D. Smith, B. Latimer, and J.P. Devlin, *J. Phys. Chem.*, **70**, 2011 (1966).
- (14) B. Moszyńska, *Acta Phys. Pol.*, **33**, 959 (1968).
- (15) B. Lunelle and C. Pecile, *J. Chem. Phys.*, **52**, 2375 (1970).
- (16) T. Takenaka, *Spectrochim. Acta*, **27A**, 1735 (1971).
- (17) M.G. Kaplunov, T.P. Panova, E.B. Yagubskii, and Yu.G. Borod'ko, *Zh. Strukt. Khim.*, **13**, 440 (1972).
- (18) A. Girlando and C. Pecile, *Spectrochim. Acta*, **29A**, 1859 (1973).
- (19) T. Takenaka, J. Umemura, S. Tadokoro, S. Oka, and T. Kobayashi, *Bull. Inst. Chem. Res., Kyoto Univ.*, **56**, 176 (1978).
- (20) J. Umemura and T. Takenaka, *Bull. Inst. Chem. Res., Kyoto Univ.*, **51**, 206 (1973).
- (21) E.B. Wilson, Jr., J.C. Decius, and P.C. Cross, "Molecular Vibrations," McGraw-Hill, New York (1955).